Journal of Power Sources 196 (2011) 1055–1060

Contents lists available at ScienceDirect

Journal of Power Sources

journal homepage: www.elsevier.com/locate/jpowsour

New process for high temperature polybenzimidazole membrane production and its impact on the membrane and the membrane electrode assembly

Zhenyu Liu*, Yu-Min Tsou, Gordon Calundann, Emory De Castro

BASF Fuel Cell Inc., 39 Veronica Avenue, Somerset, NJ 08873, USA

ARTICLE INFO

Article history:
Received 25 June 2010
Received in revised form 6 August 2010
Accepted 9 August 2010
Available online 17 August 2010

Keywords:
Polybenzimidazole
High temperature membrane
Fuel cells
MEA

ABSTRACT

Water addition is a key step in the new process developed at BASF Fuel Cell Inc. (BFC) for polybenzimidazole (PBI) membrane production. The added water prevents further polymerization and controls the solution viscosity for easier membrane casting. For large-scale PBI membrane production, a certain amount of tension is necessary during membrane upwinding. The applied tension could affect the polymer orientation and result in anisotropic membrane mechanical properties and proton conductivity. The membrane prepared with tension shows higher elastic modulus and proton conductivity in machine direction, which might suggest some degree of polymer chain orientation. However, the membrane electrode assembly (MEA) performance is not affected by the membrane's apparent anisotropic character. However, we observed performance variation as a function of MEA break-in condition, which might be explained by the formation of a phosphate anion concentration gradient during MEA operation.

1. Introduction

Use of phosphoric acid doped polybenzimidazole (PBI) for a high temperature proton exchange membrane (PEM) fuel cell was first proposed by Wainright et al. [1]. After extensive development and characterization done since then, fuel cells based on PBI membranes have been successfully commercialized.

Operation of a polymer electrolyte membrane (PEM) fuel cell at elevated temperatures (150–200 °C) has significant advantages including relief of CO poisoning of the catalyst and simplified water management. The PBI-based membranes have shown good proton conductivity [2], excellent thermal stability [3], low gas permeability [4] and acceptable oxygen reduction kinetics [5–7] in use in high temperature PEM-based fuel cells. Good fuel cell performance and durability with PBI membranes have been confirmed in recent research [8–10] and commercial activities [11]. A detailed summary of PBI-based high temperature PEM fuel cells can be found in a recent review [12].

PBI membrane can be prepared in different ways. The membrane using commercially available PBI is often cast from a PBI solution in an aprotic solvent such as N,N-dimethylacetamide (DMAc). The membrane from this process is then doped with phosphoric acid. However, the acid doping process is slow and not very uniform and thus is a difficult process to use commercially. Pemeas GmbH (now part of the BASF Fuel Cell Inc.) and Rensselaer Polytechnic Institute developed an effective and simple process using polyphosphoric acid (PPA) to produce PBI gel membranes for PEM fuel cells [13–15]. In this process, the PBI is synthesized from 3,3′,4,4′-tetraaminobiphenyl (TAB) and terephthalic acid (TPA). Polyphosphoric acid is used as polycondensation solvent, and membrane casting solvent. The intermediate PBI membranes thus cast are 'gelled' in a hydrolysis step to form the final membrane with a very high loading of phosphoric acid.

The PPA membrane process is an efficient method of membrane preparation and is very suitable for commercial scale-up. However, the PBI–PPA solution must be cast at elevated temperature, e.g. 150–180 °C. Even in this temperature range, the solution viscosity is still an order of magnitude higher than that of the PPA of the same concentration at room temperature [16]. The high viscosity of the PBI–PPA solution results in solution transport and filtration problems, and makes membrane quality control difficult.

BASF Fuel Cell Inc. (BFC) recently modified the PBI–PPA membrane process and successfully employed it at the BFC facility at Somerset, New Jersey. The polymerization reaction is monitored and controlled by agitator torque energy measurement. Harris and Walczyk reported the correlation between the solution's kinematic viscosity and the PBI polymer's inherent viscosity (IV) [16]. Their results could be used for precise control of the polymer IV. A key step in this process is the addition of water after the polymerization has reached a given torque value. The added water prevents further polymerization and the solution viscosity is thus stabilized for the membrane casting process. In fact, the solution viscosity is significantly reduced by the water addition and this allows for easier solution transport and better membrane quality control.

* Corresponding author. Tel.: +1 732 545 5100x4163; fax: +1 732 545 5170.
E-mail address: zhenyu.liu@basf.com (Z. Liu).

0378-7753/$ – see front matter © 2010 Elsevier B.V. All rights reserved.
doi:10.1016/j.jpowsour.2010.08.026

It has been reported that the PBI membranes prepared with different processes show different properties. For example, the PBI membranes cast from DMAc and doped in phosphoric acid are mechanically stronger than the membranes directly cast from the trifluoroacetic acid (TFA) phosphoric acid mixture; the doped membranes however show lower proton conductivity. We have found the membrane samples from the BFC's casting line show some anisotropic physiochemical properties. It seems that the anisotropy is the result of membrane handling after casting, likely the tension required to draw the membrane through the hydrolysis bath. In this paper, we report the effects of the anisotropic properties found in PBI membranes made in the PPA process, and the initial single cell performance of the MEAs made with these membranes.

2. Experimental

The schematic of the PBI–PPA process, solution preparation, membrane casting and membrane hydrolysis is shown in Fig. 1. The polymerization rate is controlled by the reactor temperature. After polymerization is significantly slowed by reducing reactor temperature, a quantity of water is slowly pumped into the stirred reactor to completely stop the polymerization. The solution viscosity is also reduced to allow for easier membrane casting.

The membrane is cast between 150 and 180 °C. This temperature is lower than that used in the laboratory research activities [17]. A computer guided blade provides good membrane thickness control. The 'membrane' at this step is in fact a viscous PBI–PPA solution with uniform thickness and width rather than the final hydrolyzed gelled membrane.

In the hydrolysis phase, the cast membrane is transported into the hydrolysis bath containing aqueous phosphoric acid to initiate hydrolysis of the polyphosphoric acid casting solvent. Part of the PPA in the membrane is simply displaced by aqueous acid during this step. The phosphoric acid concentration in the hydrolysis bath is in situ monitored and controlled. The hydrolyzed membrane becomes a stand-alone gel membrane and may be wound on a core. At this point, the acid concentration in the membrane is very close to that of the hydrolysis bath. While the membrane is supported on a PET carrier web, it experiences some degree of machine direction draw-down as it passes over the rolls of the hydrolysis bath. Both the membrane casting and the hydrolysis steps are continuous processes maintained at constant web speed.

The polymer's inherent viscosity has been used to evaluate the PBI polymerization process control. The isolated dry PBI is dissolved in concentrated sulfuric acid with PBI concentration of 0.1 g dL^{-1}. The solution viscosity was measured by Lauda viscosity meter and is compared to that of the sulfuric acid with same concentration.

The membrane mechanical properties and proton conductivities were determined as additional quality control measures. The membrane's mechanical properties in both the machine direction (MD) and the transverse direction (TD) are tested using Zwick 100 tensile test stand. The tests are conducted under room temperature without additional relative humidity (RH) control with laboratory relative humidity at about 50–60%. The proton conductivities in MD and TD directions are measured by Zahner electrochemical stand using an in-house customized 4-probe test cell which is similar to that used by Xiao et al. [17]. To simulate fuel cell operation conditions, the proton conductivity is measured under approximately 2% relative humidity, close to the actual relative humidity seen by the MEA in a fuel cell operating at 160–180 °C with cathode air flow at 2.0 stoichiometry. The test cell is placed in a vacuum oven for relative humidity control. Before measurement, the sample is dried at 190 °C for 1 h. The relative humidity is controlled by water introduction into the oven.

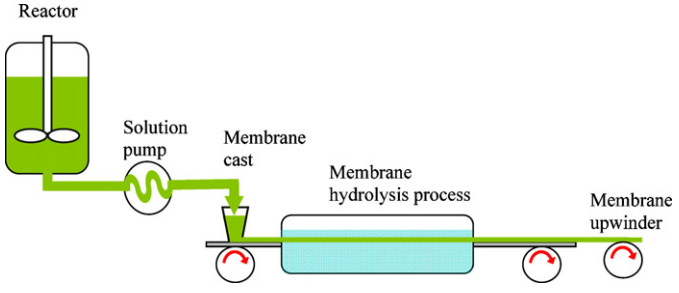

Fig. 1. Schematic of the PBI solution preparation and the membrane casting.

The MEA performance is one of the standard tests for membrane quality control at BFC. The test conditions are 180 °C under ambient pressure using dry fuel and air. The stoichiometry is 1.2 for pure hydrogen; and is 1.43 for a synthetic reformate of composition: 2.1% CO, 70% H_2, and 27.9% CO_2. The corresponding stoichiometries for air are 2.0 with hydrogen and 5.0 with reformate. The tests were carried out in a 50 cm^2 single cell with graphite bi-polar plates.

To investigate the possible impact membrane anisotropy on MEA performance, two identical MEAs were prepared in an identical manner except for membrane orientation. One MEA is mounted with the membrane's machine direction parallel to the bi-polar plate's flow channels, and the other one has the membrane's machine direction perpendicular to the flow channels. The polarization curves for both hydrogen/air and reformate/air were then determined.

3. Results and discussion

3.1. Comparison between the laboratory process and the BFC process

The primary polymerization control parameters, PPA and monomer concentrations and polymerization time/temperature ramp, in the BFC process are set similar to those values used in laboratory scale. Weber number analysis indicates that use a larger scale agitation system, the mixing condition in the BFC's reactor vessel would be much better than that seen in small laboratory reactors. Thus, synthesis of PBI polymer with higher inherent viscosities became more feasible. Further, and based on the work of Harris and Walczyk [16], the correlation of agitator torque at constant revolution with solution viscosity and thus the PBI polymer's inherent viscosity was established. This correlation allowed use of agitator torque as a key tool for polymerization control.

A novel step in the BFC's process uses water addition to stop the polymerization and to control the polymer solution viscosity. This is critical for membrane quality control. Many membrane potential defects such as bubbles, thickness non-uniformities, and particulate impurities are closely related to the difficulties in handling highly viscous solution. One can speculate that during polymerization, the hydrogen bonds formed between the protonated PBI polymer and the polyphosphoric acid, reducing polymer and acid mobility and resulting in significant solution viscosity. However, solution viscosity decreases instantaneously on water addition. The agitator torque response to the water addition is shown in Fig. 2.

The maximum amount of water introduced to the solution must be controlled to avoid possible polymer gel formation since the more dilute PPA is a somewhat poorer solvent for the PBI [17]. But a minimum amount of water addition is required to prevent further polymerization as the solution residence time in the reactor and transport lines can be hours during membrane casting. Within these limits, the process can be optimized to balance the membrane cast temperature, transport line pressure, and water addition flow rate. Internal QC showed that the membrane produced in this pro-

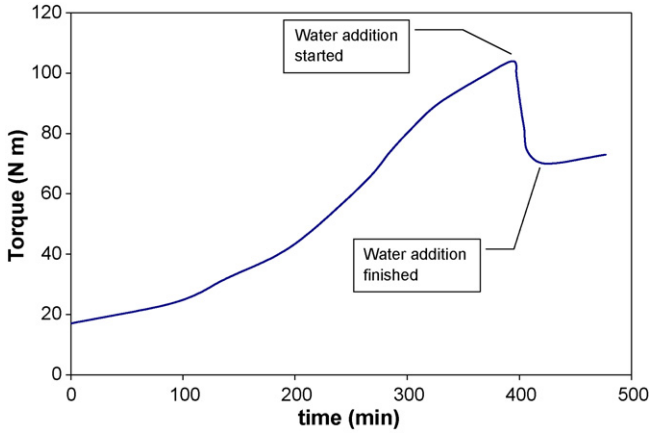

Fig. 2. The agitator torque response to the polymerization and the water addition.

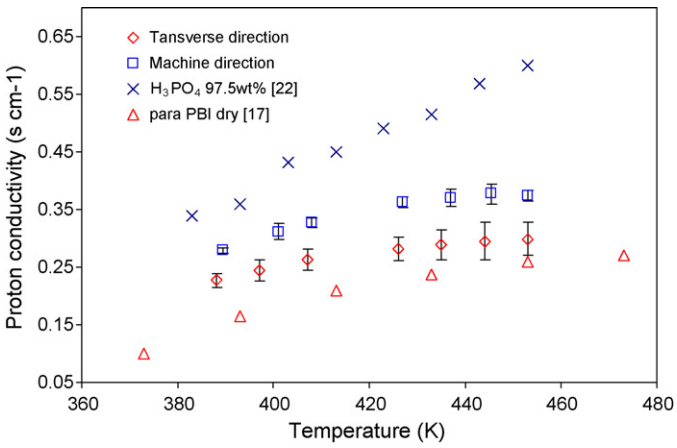

Fig. 3. Proton conductivities of PBI membranes made in the BFC process under approximately 2% relative humidity.

cess has little variation in polymer IV from beginning to end of the membrane casting, a period of about 6 h.

On hydrolysis, the clear membrane changes color quickly green to brown. The viscous solution 'membrane' becomes a tough gel membrane after the color change, which indicates a rapid transformation from solution to gel as the PPA solvent is hydrolyzed to a phosphoric acid non-solvent. This fast PPA hydrolysis and bath displacement of PPA in the membrane suggests that the acid concentration in the membrane and in the hydrolysis bath reach equilibrium in a relatively short time. The final gel membrane acid content is controlled to be about 30 phosphoric acids per PBI repeat unit. In this hydrolysis process, membrane experiences significant acid loss resulting in a large dimension change in thickness and width, but not in the machine (cast) direction. These dimensional changes on casting suggest that the morphology and structure of the polymer might have been affected with consequent membrane proton conductivity and mechanical properties anisotropy.

3.2. Mechanical properties of the membrane

The membrane tensile tests were conducted on both machine and transverse directions. Samples of different thickness were tested. All samples showed polymer IV in the range of 5.0–5.5 dL g^{-1} (0.1 g PBI per dL H_2SO_4). Membrane dimension change after hydrolysis is typically about 20% shrinkage in width and thickness, with shrinkage in the machine direction generally negligible. The tension in the machine direction is controlled by a weight applied in membrane upwinding.

Listed in Table 1 are the samples thickness, test direction, applied weight and corresponding tension, the tensile strength and the elastic modulus. All samples showed the range of elongation between 150 and 250%, and the phosphoric acid content was about 30 H_3PO_4 per PBI repeat unit. The tensile strength data were generally consistent with literature reported values [17]. It appears that tensile strength may not be affected by the applied tension in hydrolysis process. This was not surprising as the membrane tensile strength would be mainly determined by the polymer average molecular weight, measured as polymer IV in this study. The membrane's elastic modulus was however significantly affected. It seemed from Table 1 that the elastic modulus in machine direction was very sensitive to the tension applied in hydrolysis process. It generally increased with degree of tension. For example, the elastic modulus in the machine direction increased more than 30% when the tension was doubled for 600 μm thick membrane. The elastic modulus in transverse direction was substantially lower than that of the machine direction. This suggests that PBI polymer chain orientation and interactions might be affected by tension in the machine direction.

With membrane tension, polymer chain orientation may occur in the machine direction after PPA hydrolysis and it is likely that this alignment maintains on membrane take-up on a core. Correspondingly, the finished gel membrane showed substantially higher elastic modulus in the machine direction. Tensile strength on the other hand, mainly affected by the polymer average molecular weight, would not be expected to be so influenced.

3.3. Proton conductivity of the membrane

Extensive proton conduction mechanism studies with different approaches have been reported in the literature [2,18–20]. It has been well accepted that the proton conduction in phosphoric acid doped PBI or the type of phosphoric acid–PBI gel membrane described here follow the Grotthus mechanism. The excess phosphoric acid after maximum protonation of the PBI works similar to concentrated phosphoric acid, and is the main contributor to proton conductivity. Compared to liquid phosphoric acid, the acid doped PBI membranes or gel membranes have lower conductivities since proton transport has been partially interrupted by polymer.

The membrane proton conductivity data in both machine and transverse directions are shown in Fig. 3. These data were obtained under approximately 2% relative humidity in order to simulate typical fuel cell operating conditions. The proton conductivities in the machine direction were roughly 25% higher than those in the trans-

Table 1
The mechanical properties of the PBI membrane made in the BFC process.

Membrane thickness (μm)	Force/upwinder weight (kg)	Applied tension (MPa)	Elastic modulus (MPa)		Break tensile (MPa)	
			MD	TD	MD	TD
411	1	0.06	2.24 ± 0.22	1.40 ± 0.18	1.68 ± 0.28	1.24 ± 0.10
433	5	0.31	3.52 ± 0.14	1.85 ± 0.12	1.56 ± 0.21	1.11 ± 0.21
600	5	0.22	2.44 ± 0.36	1.70 ± 0.29	1.37 ± 0.16	1.17 ± 0.10
594	10	0.45	3.18 ± 0.23	1.58 ± 0.33	1.39 ± 0.23	1.08 ± 0.12

Table 2
Proton conductivities of the concentrated phosphoric acid calculated from the membrane data.

Temperature (°C)	115	125	135	154	164	172	180
Calculated from MD (s cm^{-1})	0.34	0.38	0.40	0.44	0.45	0.46	0.45
Calculated from TD (s cm^{-1})	0.27	0.30	0.32	0.34	0.35	0.36	0.36
97.5 wt% H_3PO_4 (s cm^{-1}) [22]	0.35	0.40	0.44	0.50	0.54	0.57	0.60

verse direction. The data suggested that the proton transfer and acid movement in the machine direction might be more facile. The proton conductivities in both directions were higher than the data obtained at same temperature under dry conditions [17]. It was also noticed that for temperatures higher than 150 °C, proton conductivity increased less with increasing temperature. This effect is attributed to the negative impact of the generation of pyrophosphoric acid [2].

The Bruggeman equation $\sigma = \sigma_0 \varepsilon^{\tau}$ was used to estimate the impact of the volume fraction of the phosphoric acid in the membrane. The volume fraction of phosphoric acid was roughly 0.9 for a H_3PO_4/PBI repeat unit ratio of 30. Its concentration would be about 97.5 wt% at equilibrium under 2% RH [21]. The tortuosity was assumed to be 1.8. The proton conductivities of the phosphoric acid at this concentration calculated from the Bruggeman equation using membrane data were compared with literature reported data [22] in Table 2. Note that the calculated acid proton conductivity using machine direction data showed a relatively good fit to the reported value. For example, the proton conductivity of 97.5 wt% H_3PO_4 at 150 °C was calculated to be 0.44 s cm^{-1}, which compares closely to the value 0.50 s cm^{-1} reported by Chin and Chang [22]. However, the calculations based on the proton conductivities measured in transverse direction show large variation from literature reported data.

It was reported that phosphoric acid proton conductivity decreases with addition of small molecules due to viscosity increase and acid chain interruption [23]. Similarly, PBI polymer chains would be expected to interfere with the integrity of the phosphoric acid network making proton transfer and acid molecular movement more difficult. Given PBI orientation in the casting process, the phosphoric acid network integrity in the machine direction may be less disrupted, which could account for the observed superior conductivity of the membrane's cats direction. Thus, proton conduction in the machine direction might be locally closer to that determined in concentrated phosphoric acid. Polymer chain acid interference in the transverse direction shows a more typical impact on conductivity and, as a result, the proton conductivity in that direction was correspondingly lower. For doped PBI membranes with a lower acid content, e.g. doped membrane cast from DMAc or TFA, the phosphoric acid network integrity would be significantly disrupted due to a high volume fraction of the polymer. For such membranes, the phosphoric acid network integrity would have a major impact on proton conductivity. The Bruggeman equation may not longer be applicable for these compositions.

The proton conductivities in both MD and TD directions, as well as under dry conditions have shown the same trend with temperature change. The Arrhenius plot of the Ln(σT) vs. the inverse of temperature from the Arrhenius equation, $\sigma T = \sigma_0 \exp(-Ea/RT)$ are plotted in Fig. 4. All lines showed similar activation energy, between 10 and 15 kJ mol^{-1}. According to Ma et al. [2], for high acid level PBI membranes, the energy required for optimum acid hydrogen bond orientation enabling facile proton transfer was similar. Again, for the low acid content membranes, proton movement within the acid hydrogen bridge network is partially impeded.

3.4. Single cell MEA tests

MEA performance is apparently unaffected by a somewhat anisotropic membrane. This is anticipated since membrane resistance is driven primarily by through-plane conductivity rather than in-plane conductivity. On the other hand, about 95 wt% of the membranes described here is phosphoric acid. The polymer only account for approximately 6% volume fraction of the membrane. After MEA assembly, a fraction of the membrane's phosphoric acid has been pressed into the electrode's porous structure to create the three-phase boundaries. The membrane thickness in the MEA after compression is approximately 50–75 μm.

MEA performances using hydrogen/air and reformate/air with different MEA mounting orientations are plotted in Fig. 5(a) and (b). These MEAs were prepared with identical electrodes and were controlled under identical break-in conditions before measuring polarization curves. Thus, no MEA performance difference was observed for MEAs mounted with their membrane machine direction parallel or perpendicular to the flow channels of the bi-polar plates. The data confirm that MEA performance is unaffected by the anisotropic membranes described.

MEA performances could vary with MEA 'break-in' conditions. This may be attributed to a phosphate anion concentration gradient within the MEA which forms during cell operation. In our preliminary study, the polarization curves were recorded after subjecting the cell to different brake-in conditions; the cells were operated at constant current density of 0.2 and 0.6 A cm^{-2} overnight. These polarization curves are plotted in Fig. 6(a) for hydrogen fuel, and (b) for reformate fuel. The performance differences at low current density were negligible in both cases. However, the cell broken-in at 0.6 A cm^{-2} was 20 mV at 1 A cm^{-2} lower than the cell broken-in at 0.2 A cm^{-2} with either hydrogen or reformate fuel. This behavior was reversible in that both cells at this point would show the same polarization curves when reconditioned at same current density, e.g. 0.2 A cm^{-2}.

Under operation, the phosphate anion would migrate toward higher potential once the potential gradient is formed across the MEA. Phosphoric acid, 95 wt% acid concentration in the MEA, self-dissociates as $2H_3PO_4 \rightarrow H_2PO_4^- + H_4PO_4^+$. This self-dissociation is in fast equilibrium [21]. However, when water is introduced into the system, i.e. generated at cathode under operation, the $H_4PO_4^+$ may be expected to further dissociate into phosphate anion as $H_4PO_4^+ + 2H_2O \rightarrow H_2PO_4^- + 2H_3O^+$. In addition, the undissociated phosphoric acid may also combine with water to form phosphate

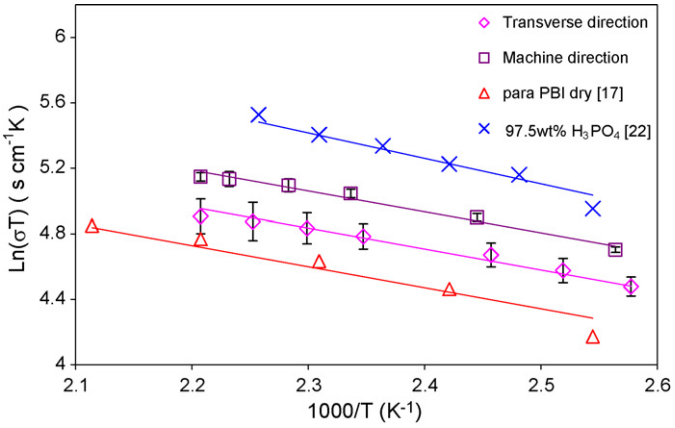

Fig. 4. The Arrhenius plot of the proton conductivities of PBI membranes made in the BFC process.

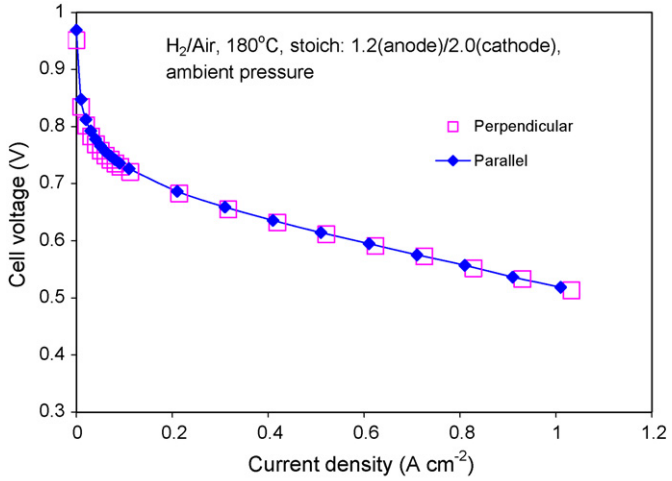

(a) Polarization curves of MEAs operated with H_2/air

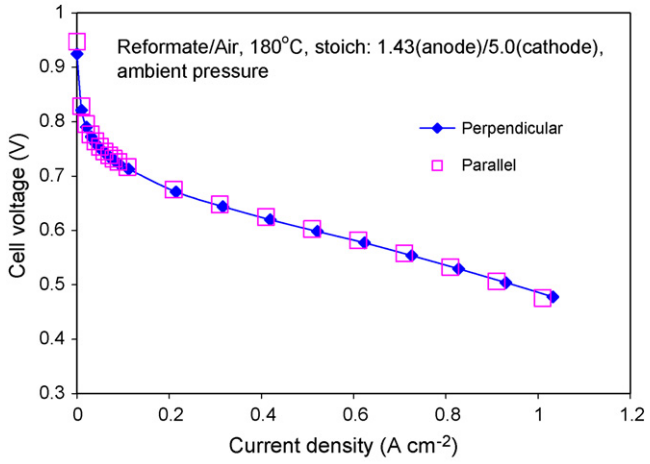

(b) Polarization curves of MEAs operated with reformate/air

Fig. 5. Polarization curves of MEAs using PBI membranes made in the BFC process. MEAs were mounted with membrane machine direction parallel (labeled as parallel) or perpendicular (labeled as perpendicular) to the flow field channels of the bipolar plates. Polarization curves were obtained after identical break-in conditions. (a) Polarization curves of MEAs operated with H_2/air. (b) Polarization curves of MEAs operated with reformate/air.

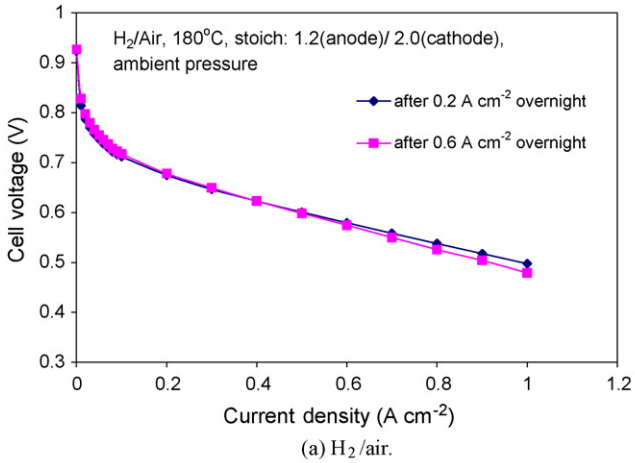

(a) H_2/air.

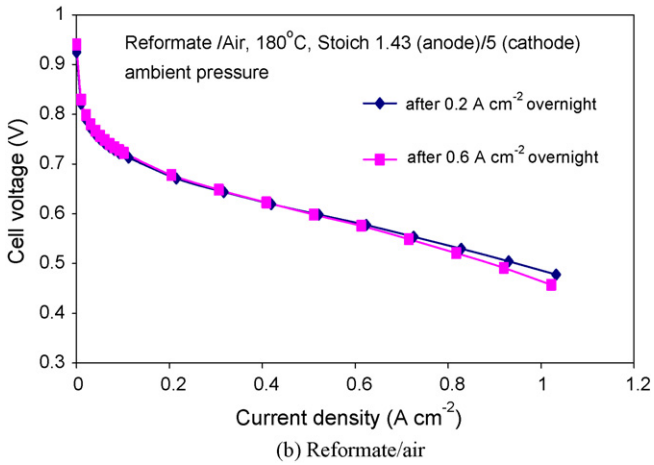

(b) Reformate/air

Fig. 6. Polarization curves obtained after different break-in conditions. (a) H_2/air. (b) Reformate/air.

anions, i.e. $H_3PO_4 + H_2O \rightarrow H_2PO_4^- + H_3O^+$ ($pK_a = 2.16$). Therefore, the phosphate anion concentration increases with water content. In our experiments, the MEA operated at 0.6 A cm^{-2} would have a higher phosphate anion concentration than that operated at 0.2 A cm^{-2}.

Water generation at the cathode is proportional to current density. The polarization curves plotted in Fig. 6(a) and (b) indicate that both 0.2 and 0.6 A cm^{-2} are within the ohmic region. Hence for the cathode, it is expected that the local current density at the catalyst layer/membrane interface could be the highest. It decreases across the catalyst layer and reaches its minimum at the catalyst layer/gas diffusion layer (GDL) interface. The study of the fuel cell cathode showed that the current distribution across the catalyst layer would be less uniform for the MEA operated at a higher current density [24]. It is expected that the water concentration gradient formed in the cathode forms in a similar manner. Cathode generated water could diffuse toward the anode and dissociate the local phosphoric acid. The non-uniform current distribution and the associated water concentration gradient suggest the existence of a phosphate anion concentration gradient across the MEA. This would be affected by the local water concentration as well as the potential gradient. Further, the phosphate anion gradient would result in additional voltage loss. The MEA operated at higher current density will have less uniform phosphate anion distribution in the through-plane direction. It has been reported that the transport number of the anions in H_3PO_4–H_2O system is very low (about 0.01 for 70 wt% acid) [25]. Jayakody et al. recently showed the phosphate anion self-diffusion coefficient in PBI membrane is at least two orders of magnitude lower than that of the proton (in the order of 10^{-5} cm^2 s^{-1} at 180 °C) [26]. These studies suggested that the polarization curves, which were obtained by recording voltage at each current density for a short period of time, may have been too rapid to allow the phosphoric acid dissociation and the phosphate anion distribution to reach new equilibria at each test point. Thus, variations at high current density region could be observed as the potential gradient was relatively high.

4. Conclusions

A new PBI membrane production line using modified PBI–PPA gel membrane process has been constructed at the BASF Fuel Cell Inc., facility in Somerset NJ. In large-scale production, certain degree of tension is necessary for membrane take-up on a core. It has been found that the membrane mechanical properties and proton conductivity are affected by the applied tension. The membrane's mechanical properties and proton conductivity are somewhat anisotropic. Higher membrane elastic modulus and proton conductivity have been observed in machine direction. It suggests that the PBI polymer morphology might be affected and

the polymer chain might be oriented in the machine direction. Membrane anisotropy improves the elastic modulus in machine direction, and reduces the negative impacts of dissolved PBI on proton transfer and acid movement in that direction.

Single cell MEA tests showed that the membrane anisotropic properties do not affect MEA performance. MEA performance varies cell break-in conditions and these variations suggest the possible formation of a phosphate anion gradient under operation.

References

[1] J.S. Wainright, J.T. Wang, D. Weng, R.F. Savinell, M.H. Litt, J. Electrochem. Soc. 142 (1995) L121–L123.
[2] Y. Ma, J.S. Wainright, M.H. Litt, R.F. Savinell, J. Electrochem. Soc. 151 (2004) A8–A16.
[3] S.R. Samms, S. Wasmus, R.F. Savinell, J. Electrochem. Soc. 143 (1996) 1225–1232.
[4] D. Weng, J.S. Wainright, U. Landau, R.F. Savinell, J. Electrochem. Soc. 143 (1996) 1260–1263.
[5] K.C. Neyerlin, A. Singh, D. Chu, J. Power Sources 176 (2008) 112–117.
[6] S.K Zecevic, J.S. Wainright, M.H. Litt, S.L. Gojkovic, R.F. Savinell, J. Electrochem. Soc. 144 (1997) 2973–2982.
[7] Z. Liu, J.S. Wainright, M.H. Litt, R.F. Savinell, Electrochim. Acta 51 (2006) 3914–3923.
[8] T.J. Schmidt, J. Baurmeister, ECS Trans. 3 (2006) 861–869.
[9] S. Yu, L. Xiao, B.C. Benicewicz, Fuel Cells 8 (2008) 156–174.
[10] J. Mader, L. Xiao, T.J. Schmidt, B.C. Benicewicz, Adv. Polym. Sci. 216 (2008) 63–124.
[11] Fuel Cell Bull. 2 (2006) 12–15.
[12] Q. Li, J.O. Jensen, R.F. Savinell, N.J. Bjerrum, Prog. Polym. Sci. 34 (2009) 449–477.
[13] G. Calundann, M.J. Sansone, O. Uensal, J. Kiefer, PCT Int. Appl. (2002), WO 2002081547.
[14] G. Calundann, B. Benicewicz, J. Baurmeister, PCT Int. Appl. (2004), WO 2004030135.
[15] J. Kiefer, O. Uensal, G. Calundann, et al., PCT Int. Appl. (2004), WO 2004024796.
[16] T.A. Harris, D. Walczyk, J. Appl. Polym. Sci. 111 (2009) 1286–1292.
[17] L. Xiao, H. Zhang, E. Scanlon, L.S. Ramanathan, E. Choe, D. Rogers, T. Apple, B.C. Benicewicz, Chem. Mater. 17 (2005) 5328–5333.
[18] C.E. Hughes, S. Haufe, B. Angerstein, R. Kalim, U. Mahr, A. Reiche, et al., J. Phys. Chem. 108 (2004) 13626–13631.
[19] R. Bouchet, S. Miller, M. Duclot, J.L. Souquet, Solid State Ionics 145 (2001) 69–78.
[20] R. He, Q. Li, G. Xiao, N.J. Bjerrum, J. Membr. Sci. 226 (2003) 169–184.
[21] S. Sarangapani, P. Bindra, E. Yeager, Physical and Chemical Properties of Phosphoric Acid, US DOE Final Report, 1981.
[22] D.T. Chin, H.H. Chang, J. Appl. Electrochem. 19 (1989) 95–99.
[23] A. Schechter, R.F. Savinell, Solid State Ionics 147 (2002) 181–187.
[24] Z. Liu, Ph.D. Thesis, Case Western Reserve University, Cleveland, OH, 2004.
[25] D. Weng, Ph.D. Thesis, Case Western Reserve University, Cleveland, OH, 1996.
[26] J.R.P. Jayakody, S.H. Chung, L. Durantino, H. Zhang, L. Xiao, B.C. Benicewicz, S.C. Greenbaum, J. Electrochem. Soc. 154 (2007) B242–B246.